

Underlying mechanisms for normal heat transport in one-dimensional anharmonic oscillator systems with a double-well interparticle interaction

Daxing Xiong[†]

Department of Physics, Fuzhou University, Fuzhou 350108, People's Republic of China

E-mail: phyxiongdx@fzu.edu.cn

Abstract. Previous studies have suggested a crossover from superdiffusive to normal heat transport in one-dimensional (1D) anharmonic oscillator systems with a bounded double-well type interatomic interaction like $V(\xi) = -\xi^2/2 + \xi^4/4$, when the system temperature is varied. In order to well understand this unusual manner of thermal transport, here we investigate in detail how the spreading processes of three physical quantities, i.e., the heat, the total energy, and momentum, would depend on temperature. We find that three main points are worth noting: (i) The crossover from superdiffusive to normal heat transport has been well verified from a new perspective of heat spreading; (ii) The spreading of the total energy is found very distinct from heat diffusion, especially that under some temperature regimes energy is strongly localized, while heat can be superdiffusive. So one should take care to derive a general connection between heat conduction and energy diffusion; (iii) In a narrow range of temperatures, the momentum spreading indicates clear viscosity; however, the viscosity can not be directly used to understand the normal transport of heat. An analysis of phonons spectra suggests that we should also take the effects of phonons softening into account. All of these results may provide insights into establishing the connection between the macroscopic heat transport and the underlying dynamics in 1D systems.

PACS numbers: 05.60.-k, 44.10.+i

[†] Author to whom any correspondence should be addressed.

1. Introduction

The viewpoint of anomalous heat transport in one-dimensional (1D) momentum conserved systems has now been widely accepted [1, 2]. The anomaly means that the “standard” heat transport law, i.e., the Fourier’s law of heat conduction, stating that, the heat flux \mathbf{J} is proportional to the temperature gradient ∇T : $\mathbf{J} = -\kappa \nabla T$, with κ the heat conductivity assumed to be constant, is not validated. In particular, for 1D anharmonic oscillator systems with conserved momentum and symmetric interparticle interactions, it has now been generally believed that κ is not a constant but follows a simple space L scaling $\kappa \sim L^\alpha$ [1, 2]. (For the momentum-conserving systems with asymmetric interactions, refer to the recent progress [3, 4] and debates [5, 6, 7, 8]). Despite that there is still no consensus on the universality classes of the scaling exponent α and its accurate value(s), in most cases $0 < \alpha < 1$ [9, 10, 11, 12, 13, 14, 15, 16] can be concluded. This power-law space scaling has also been corroborated by some relevant experimental studies of carbon nanotubes [17].

Nevertheless, there are still two exceptional systems with both conserved momentum and symmetric interactions against the above belief, i.e., the 1D coupled rotator system and the chain with a double-well (DW) potential. For both systems a transition (or crossover) from superdiffusive to normal heat transport (obeys the Fourier’s law, $\alpha = 0$) has been claimed to take place. Several mechanisms have been proposed to understand the observed normal transport in rotator systems. Early works related the mechanism to the occurrence of phase jump [18] and the excitation of high-frequency stationary localized rotational modes [19]. While quite recently the mechanism has been traced back to the viscosity indicated from momentum diffusion [20] and the absence of the conserved quantity of stretch from the perspective of nonlinear fluctuation hydrodynamics [21, 22]. However, when one turns to the bounded DW system, the underlying mechanism of normal transport has not yet been clarified so far. Even worse, whether the transport would be normal or abnormal remains controversial: early results indicated that heat conduction is normal at low temperatures [18], nevertheless it was doubted later by [1, 2]. Two recent works revisited the issue and suggested that normal behavior may appear in a narrow temperature region near $T \simeq 0.1$ [23]. In a quite recent work, we also have shown convincing evidences for this normal behavior [24], however, the underlying mechanisms are still not very clear.

In the present work we perform a further careful examination on the unusual heat transport and its underlying mechanisms in the 1D DW oscillator systems. For this purpose we shall first focus on the heat spreading process. To study heat transport, usually the space scaling exponent α is given the most attention, for which there are now two main kinds of numerical approaches, i.e., direct nonequilibrium molecular dynamics simulations [25] and the method based on Green-Kubo formula [26]. However, just as raised by S. Olla in a discussion session of a recent workshop [27]: the studies employing both methods for deriving α usually ignored another key time scale. As concerning time scaling may involve more detailed information, which would present a more detailed

prediction of heat transport, here we shall investigate the relaxation of equilibrium heat fluctuations of the system to derive the space-time scaling to characterize the heat transport behavior. We shall explore how this space-time scaling would depend on the system temperature, through which we are able to verify that, normal transport is indeed likely to take place under certain temperature regimes.

To further understand this normal transport we shall also carefully examine the relaxation of other two physical quantities fluctuations, i.e., the total energy and momentum. We will show clear distinctions between the spreading of heat and the total energy. From the momentum spreading we will reveal the emerging of viscosity (under some temperature regimes); nevertheless, we find that this viscosity can not be directly attributed to the observed normal heat transport. A careful analysis of the system's phonons spectra indicates that, around the crossover temperature point of $T \simeq 0.1$, phonons clearly tend to become softest. Based on both facts, we further conjecture that, under the appropriate temperature, phonons softening, together with the viscosity from momentum diffusion, may result in the observed normal heat transport in DW systems.

2. Model

The focused model is a 1D oscillator system, whose Hamiltonian reads:

$$H = \sum_k \left[\frac{p_k^2}{2\mu} + V(q_{k+1} - q_k) \right], \quad (1)$$

where q_k denotes the displacement of the k th particle from its equilibrium position and p_k its momentum. The mass μ is set to unit. The potential takes the bounded DW type as

$$V(\xi) = -\xi^2/2 + \xi^4/4. \quad (2)$$

Such a system is very peculiar. First, Equation (2) is a extension of Fermi-Pasta-Ulam (FPU) interactions to the particular bounded DW type, which is usually adopted to model the structural phase transition [28]. We have plotted the order parameter $\langle q_{k+1} - q_k \rangle$, the ensemble average of adjacent particles relative displacement (from their equilibrium positions), as a function of temperature T for several space sizes L (see Figure 1) and verified that, for a potential like Eq. (2), regardless of L , there is a phase transition region around $T \simeq 0.02-0.1$. The second point worth noting is that this system does not bare linear-wave dynamics (with the unusual phonon dispersion) [29], thus whether the linear phonon dynamics would still apply should be further tested. We expect that such two unusual features may affect heat transport and to understand how they may is thus interesting.

3. Methods

To identify the space-time scaling exponent for heat transport, usually one can investigate the decay of energy pulses or the equilibrium energy fluctuations

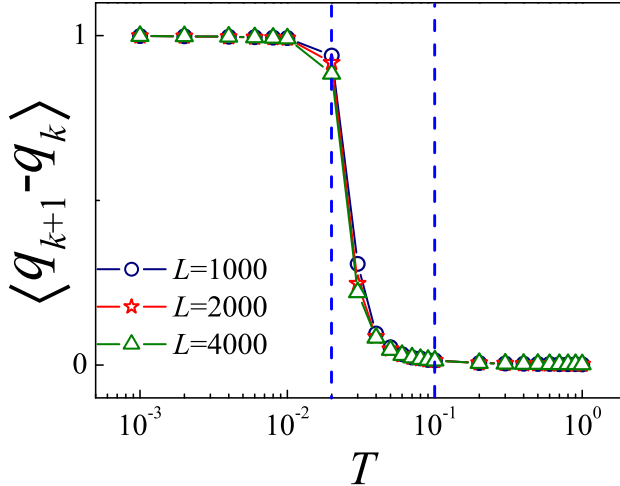


Figure 1. (Color online) Order parameter $\langle q_{k+1} - q_k \rangle$ vs temperature T , where the circles, stars and triangles correspond to the results of space size $L = 1000, 2000, 4000$; and from left to right, the vertical dashed lines denote $T = 0.02$ and $T = 0.1$, respectively.

correlation [30, 31, 32, 33, 34, 35, 36, 37]. However, studying the energy pluses decay may be unable to avoid huge statistical fluctuations [33], hence, here we apply the equilibrium correlation method for our investigations. This correlation approach was first proposed by Zhao [32] for studying the total energy fluctuations spreading and then extended to be applicable to investigate both heat and other physical quantities fluctuations decay [37]. For further detailed implementation, one can also refer to [38].

We shall mainly focus on the following three normalized spatiotemporal correlation functions of the three main physical quantities fluctuations, i.e., the heat energy, the total energy and momentum, defined as follows [32, 37]

$$\rho_Q(x, t) = \frac{\langle \Delta Q_j(t) \Delta Q_i(0) \rangle}{\langle \Delta Q_i(0) \Delta Q_i(0) \rangle}; \quad (3)$$

$$\rho_E(x, t) = \frac{\langle \Delta E_j(t) \Delta E_i(0) \rangle}{\langle \Delta E_i(0) \Delta E_i(0) \rangle}; \quad (4)$$

$$\rho_p(x, t) = \frac{\langle \Delta p_j(t) \Delta p_i(0) \rangle}{\langle \Delta p_i(0) \Delta p_i(0) \rangle}, \quad (5)$$

respectively; where $\langle \cdot \rangle$ represents the spatiotemporal average; $\Delta Q_i(t) \equiv Q_i(t) - \langle Q_i \rangle$, $\Delta E_i(t) \equiv E_i(t) - \langle E_i \rangle$, $\Delta p_i(t) \equiv p_i(t) - \langle p_i \rangle$; $Q_i(t) \equiv \sum Q(x, t)$, $E_i(t) \equiv \sum E(x, t)$ and $p_i(t) \equiv \sum p(x, t)$ denote the heat energy, the total energy and momentum densities in an equal and appropriate lattice bin i (the number of particles in the i -th bin is equal to $N_i = L/b$, where b is the total number of the bins), respectively. For any particle in each bin, $E(x, t)$ and $p(x, t)$ are the single-particle's total energy and momentum at the absolute displacement x and time t ; $Q(x, t) \equiv E(x, t) - \frac{(\langle E \rangle + \langle F \rangle)M(x, t)}{\langle M \rangle}$ [39] is the

particle's heat energy, with $M(x, t)$ the corresponding mass density function, $\langle E \rangle$ ($\langle M \rangle$) and $\langle F \rangle$ the spatiotemporally averaged energy (mass) density and the internal pressure of the system in equilibrium state, respectively. Note that to calculate our correlation functions, here we should have to discretize the space into several bins, thus the space variable should be the absolute displacement x rather than the label k of the particle. We emphasize that such a key coarse-grained procedure may significantly affect the final results [40].

The correlation functions $\rho_Q(x, t)$, $\rho_E(x, t)$ and $\rho_p(x, t)$ are employed to characterize the probability density functions (PDF) profiles of the spatiotemporal spreading of the initial physical quantities fluctuations. If these PDF profiles have been obtained, then a space-time scaling analysis may enable us to identify the corresponding transport manners.

As to our simulations, we assume the number of particles equal to the space size L , then in view of the symmetric potential of the system, the averaged pressure is fixed at zero throughout the simulations. We mainly consider two cases of space size $L = 2000$ and 4000 , which enables us to obtain an effective space size (about $L_{\text{effective}} = 500 - 1000$) for a long time up to $t = 200 - 600$ for the spreading. For each L , we apply the periodic boundary conditions, fix the bins number $b \equiv L/2$, and set the lattice constant $a \equiv 2$. We utilize the stochastic Langevin heat baths [1, 2] to thermalize the system for preparing the canonical equilibrium systems (with fixed T) and employ the Runge-Kutta algorithm of 7th to 8th order with a time step 0.05 to evolve the system. The equilibrium systems are prepared by evolving the systems for a long enough time ($> 10^7$ time units of the models) from properly assigned initial random states, then all the systems are evolved in isolation for deriving the correlation information. The size of the ensemble for deriving the correlations is about 8×10^9 .

4. Results

4.1. Heat transport

Now let us first see the heat spreading results. Figure 2 depicts the PDF profiles of $\rho_Q(x, t)$ at a typical long time $t = 600$ for four temperatures, from low to high. In view of the transition region shown in Figure 1, the lowest temperature considered here is fixed at $T = 0.02$, up to which we have verified that the final results are insensitive to the initial states assigned to just one of the potential wells, or alternately, or randomly. From Figure 2 it can be clearly seen that the shapes of the profiles under different temperatures are different: while for a low temperature $T = 0.02$ and a high temperature $T = 2.5$ one can identify one central peak and two side peaks; in some intermediate temperature ranges, such as $T = 0.05$ and $T = 0.1$, the side peaks seem to disappear. Thus, the latter cases of $T = 0.05$ and $T = 0.1$ look like Gaussian distributions that are usually exhibited in normal transport; while for the cases that the side peaks do not disappear, the PDF profiles are in good coincidence with Lévy walks stable distributions

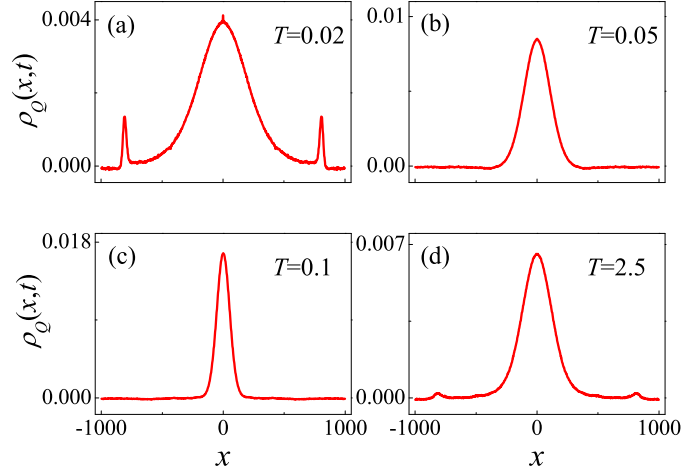


Figure 2. (Color online) $\rho_Q(x, t)$ for time $t = 600$ ($L_{\text{effective}} = 2000$) under temperatures $T = 0.02$ (a); $T = 0.05$ (b); $T = 0.1$ (c) and $T = 2.5$ (d), respectively.

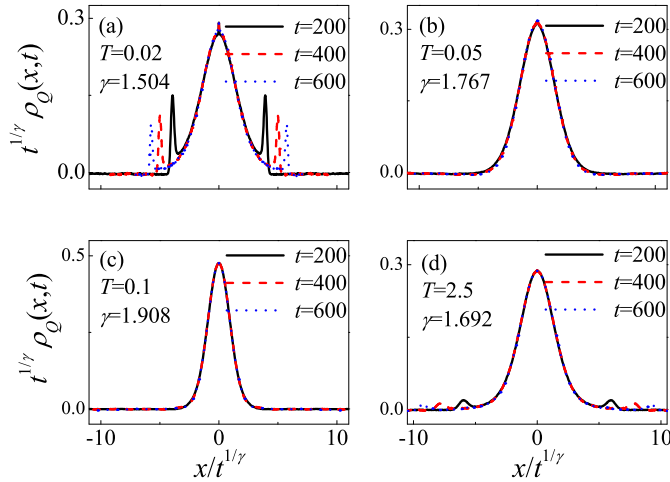


Figure 3. (Color online) Rescaled $\rho_Q(x, t)$ shown in Fig. 2: (a) $T = 0.02$ ($\gamma = 1.504$); (b) $T = 0.05$ ($\gamma = 1.767$); (c) $T = 0.1$ ($\gamma = 1.908$); and (d) $T = 2.5$ ($\gamma = 1.692$), respectively. In each curve scaling $t^{1/\gamma} \rho(x, t)$ vs $x/t^{1/\gamma}$ for three different times are compared.

for describing superdiffusive transport [41].

Viewing this coincidence, we perform a Lévy scaling analysis for the PDF profiles central parts

$$\rho_Q(x, t) \simeq \frac{1}{t^{1/\gamma}} \rho_Q\left(\frac{x}{t^{1/\gamma}}, t\right), \quad (6)$$

which then enables us to identify a scaling exponent γ for precisely characterizing the heat transport process. We recall that usually $\gamma = 1$, $1 < \gamma < 2$ and $\gamma = 2$ correspond to the ballistic, superdiffusive, and normal transport, respectively.

After obtaining the scaling exponent with formula (6), in figure 3 we plot the rescaled $\rho_Q(x, t)$ for four typical temperatures focused in Figure 2, from which it can be seen that, for all temperature cases, formula (6) is beautifully satisfied suggesting that the focused systems heat spreading can be well captured by the single-particle's Lévy walk models; though the scaling exponent γ is different for different temperatures: (i) for the lowest temperature $T = 0.02$, $\gamma \simeq 1.504$, in good coincidence with some theoretical predictions of $\gamma = 3/2$ for even symmetric potentials [42, 43, 44]; (ii) in the case of high temperature $T = 2.5$, the best fitting gives $\gamma \simeq 1.692$, consistent well with the popular numerical results $\gamma = 5/3$ based on Lévy walks models [30, 31, 33, 34, 35, 36]; (iii) while in the intermediate ranges of temperature, γ tends to increase; in particular, around $T \simeq 0.1$, $\gamma \simeq 1.908$, suggesting that a heat transport process very close to normal ($\gamma = 2$) diffusion appears to take place, which is in good agreement with the early numerical findings of normal heat conduction ($\alpha \simeq 0$) under this temperature regimes [1, 18, 23].

Then what are the pictures for other T values? To answer this question we carefully examine the results of $\gamma(T)$ and summarize them in Figure 4. Therein four data points are extracted from Figure 3, while others are calculated (fitted) additionally in the same way. For each T , two long effective space size of $L_{\text{effective}} = 1000$ and 2000 have been compared for the analysis of finite size effects. From Figure 4 one can see that regardless of L , as T increases from $T = 0.02$ to $T = 2.5$, γ increases first from $\gamma \simeq 3/2$, reaches its maximum value close to $\gamma = 2$ at $T_{\text{tr}} \simeq 0.1$, then decreases down to $\gamma \simeq 5/3$ for $T = 2.5$. Thus, γ appears not a universal constant, independence of T , and a crossover from superdiffusive ($1 < \gamma < 2$) to normal transport ($\gamma = 2$) at about $T_{\text{tr}} \simeq 0.1$ is likely to take place, though longer space sizes simulations are still required to confirm the transition. This result is consistent with those reported in [23], but obviously more precise and detailed.

In addition to the central peak's scaling, it is also interesting to examine the scaling of two side peaks, the results of which are shown in Figure 5. Since under some intermediate temperature regimes the side peaks are absent, here we just employ the two temperature cases of $T = 0.02$ and $T = 2.5$ as examples. The scaling formula (proposed in [33]) that we use reads

$$\rho_Q(x, t) = \frac{1}{t^{\gamma-1/2}} \rho_Q \left(\frac{x - vt}{t^{1/2}}, t \right); |x| \equiv vt, \quad (7)$$

where γ is the scaling exponent of the central part extracted from Figure 3(a) and (d), v is the side peaks velocity, which is verified to be a constant depending on temperature and actually measured by our direct dynamic simulations with $v \simeq 1.35$ ($T = 0.02$), and $v \simeq 1.34$ ($T = 2.5$), respectively. From Figure 5 it can be clearly seen that both curves show good satisfactory with the scaling formula (7), suggesting that in the 1D DW systems, the Lévy walks scaling [33, 41] is validated to heat spreading, not only for the central parts (it may correspond to heat mode in hydrodynamics), but also for the side peaks (sound modes).

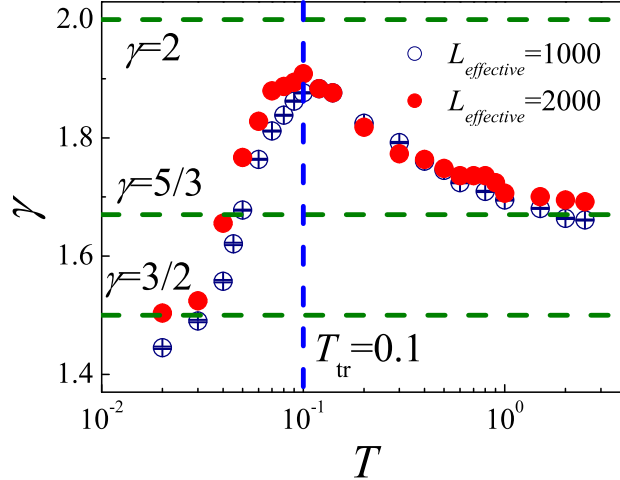


Figure 4. (Color online) γ vs temperature T , where the hollow (solid) circle corresponds to $L_{\text{effective}} = 1000$ (2000), and the horizontal dashed lines, from bottom to top, denote $\gamma = 3/2$, $\gamma = 5/3$ and $\gamma = 2$; the vertical dashed line denotes $T_{\text{tr}} = 0.1$, respectively.

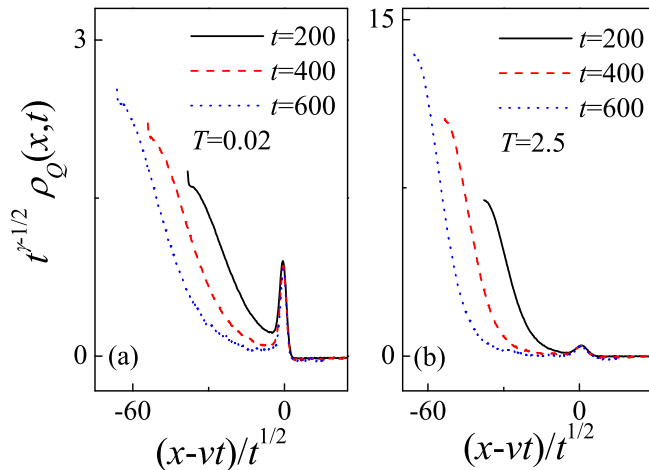


Figure 5. (Color online) Side peaks scaling: (a) $T = 0.02$ with velocity $v = 1.35$, (b) $T = 2.5$ with $v = 1.34$, respectively.

4.2. Transport of total energy

Next, we turn to the total energy's spreading. The main purpose of this section will be limited to demonstrating the distinctions between the total energy's diffusion and heat spreading. We will show that the spreading processes of these two physical quantities could be very different, thus one should take very care to relate heat conduction to just energy diffusion [45].

Figure 6 shows $\rho_E(x, t)$ for four focused temperatures the same as those in Figure

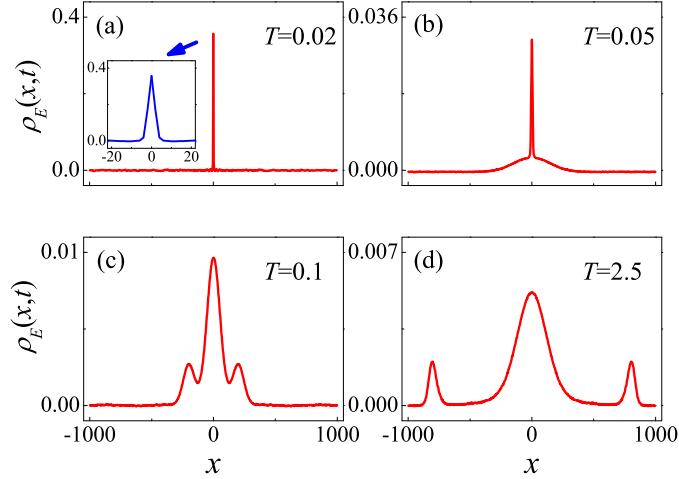


Figure 6. (Color online) $\rho_E(x, t)$ for time $t = 600$ ($L_{\text{effective}} = 2000$) under system temperatures $T = 0.02$ (a); $T = 0.05$ (b); $T = 0.1$ (c) and $T = 2.5$ (d), respectively.

2, which then enables us to make a quick comparison of the heat and the total energy spreading. From Figure 6 it can be seen that, despite in the high temperatures, $\rho_E(x, t)$ also shows one central peak and two side peaks [see Figure 6(d)], similar to $\rho_Q(x, t)$; for the cases of low temperatures, $\rho_E(x, t)$ implies very strong localizations [see Figure 6(a)]; while around the crossover temperature regimes, there is a transition from localization to delocalization for energy [see Figure 6(b)-(c)]. This phenomenon is very strange, since under some temperature regimes, the total energy is strongly localized, while heat can be superdiffusive [see Figure 2(a)], the mechanisms of which are thus interesting and we wish to understand via further studies.

Finally, we would like to note that though the difference between $\rho_Q(x, t)$ and $\rho_E(x, t)$ is slight in the frequently considered FPU- β systems (under certain appropriate temperature regimes) [37], and there previous trying to relate heat conduction to only the total energy diffusion in fact does not deviate too much; however, in the case of 1D DW systems considered here, concerning the heat spreading obviously seems more reasonable.

4.3. Momentum transport

In order to further understand the crossover manner of $\rho_Q(x, t)$, we then move to the spreading process of the third physical quantity, the momentum, since a quite recent work has attributed the normal heat transport to the viscosity from momentum diffusion [20].

Figure 7 depicts $\rho_p(x, t)$ of momentum spreading at time $t = 600$ for six temperature values, among which, four temperature cases of $T = 0.02$, $T = 0.05$, $T = 0.1$ and $T = 2.5$ are those considered in Figures. 2-3 and 6, while two additional temperatures $T = 0.03$ and $T = 0.04$ are added for further demonstrating the details of viscosity. From Figure

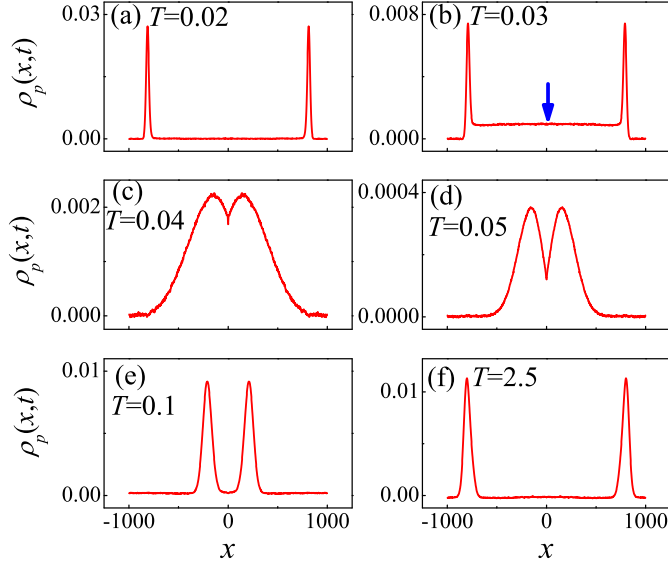


Figure 7. (Color online) $\rho_p(x, t)$ for time $t = 600$ ($L_{\text{effective}} = 2000$) under system temperatures $T = 0.02$ (a); $T = 0.03$ (b); $T = 0.04$ (c); $T = 0.05$ (d); $T = 0.1$ (e); and $T = 2.5$ (f), respectively.

7 it can be seen that, in both cases of a low and high temperature, they are ballistic momentum transport without any viscosity [see Figure 7(a) and (f)]; however, in the intermediate temperature ranges, the emerging of viscosity can be clearly identified [see Fig. 7(b)-(e)].

The viscosity from momentum spreading may be characterized by [20]:

$$\langle \Delta x_p^2(t) \rangle = \sum_x x_p^2 \rho_p(x, t) \sim t^\mu, \quad (8)$$

where $\langle \Delta x_p^2(t) \rangle$ is the mean squared deviation (MSD) of momentum spreading, μ the time scaling exponent. Following [20], usually it is assumed that $\mu = 2$ corresponds to the complete no viscosity case; while for $\mu = 1$ the profile of $\rho_p(x, t)$ may turn to a Gaussian distribution, thus implying the absolute viscosity case; $1 < \mu < 2$ then lies somewhere in between.

Figure 8 presents some typical results of the MSD $\langle \Delta x_p^2(t) \rangle$ versus t (log-log), a linear fitting of which then gives the scaling exponent μ . Indeed, in the cases of $T = 0.02$ and $T = 2.5$, our best fittings suggest that in both cases μ are very close to 2, thus supporting the ballistic momentum spreading processes; while for $T = 0.05$ and $T = 0.1$, the best fittings show $\mu \simeq 1.29$ and $\mu \simeq 1.76$, respectively. Now it is clear that if μ actually measures the viscosity, then the case of $T = 0.05$ obviously shows more viscosity than $T = 0.1$. We thus further examine μ as a function of T and summarize the result in Figure 9. As expected, it is $T_{\text{tr}} = 0.05$, rather than $T_{\text{tr}} = 0.1$ appearing to be the turning point from more viscosity to less. However this most viscosity temperature point of $T_{\text{tr}} = 0.05$ seems not directly related to the normal heat transport found around $T_{\text{tr}} = 0.1$, though it may play a role.

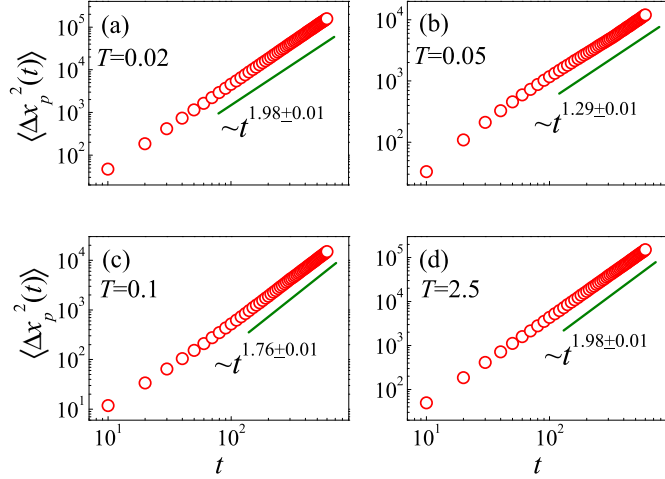


Figure 8. (Color online) $\langle \Delta x_p^2(t) \rangle$ of momentum spreading vs t for temperatures $T = 0.02$ ($\mu = 1.98 \pm 0.01$) (a); $T = 0.05$ ($\mu = 1.29 \pm 0.01$) (b); $T = 0.1$ ($\mu = 1.76 \pm 0.01$) (c), and $T = 2.5$ ($\mu = 1.98 \pm 0.01$) (d), respectively.

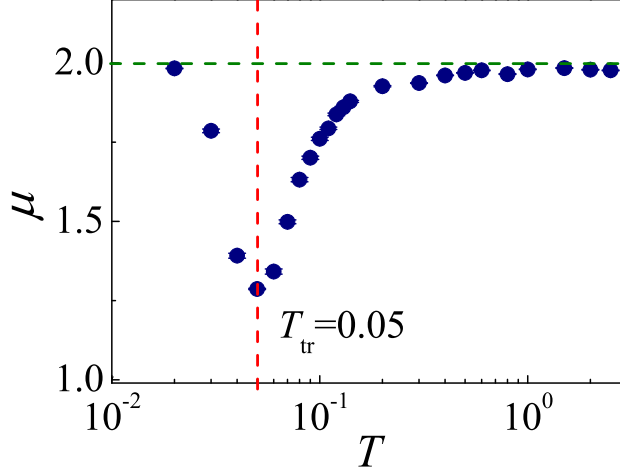


Figure 9. (Color online) Scaling exponent μ of momentum spreading vs T . The vertical (horizontal) line denotes $T_{\text{tr}} = 0.05$ ($\mu = 2$).

4.4. Phonons spectra

The above two crossover (turning) points of temperature for heat (momentum) spreading naturally puzzle us. In order to present a clearer picture, we finally turn to analyzing how the phonons spectra $P(\omega)$ of this system would depend on temperature, from which we may get some suggestive information.

Figure 10 depicts $P(\omega)$ vs T for six typical temperatures focused in Figure 7. For each temperature, we calculate $P(\omega)$ by applying a frequency analysis of the equilibrium states particles velocity along the systems. From Figure 10 it can be seen that $P(\omega)$

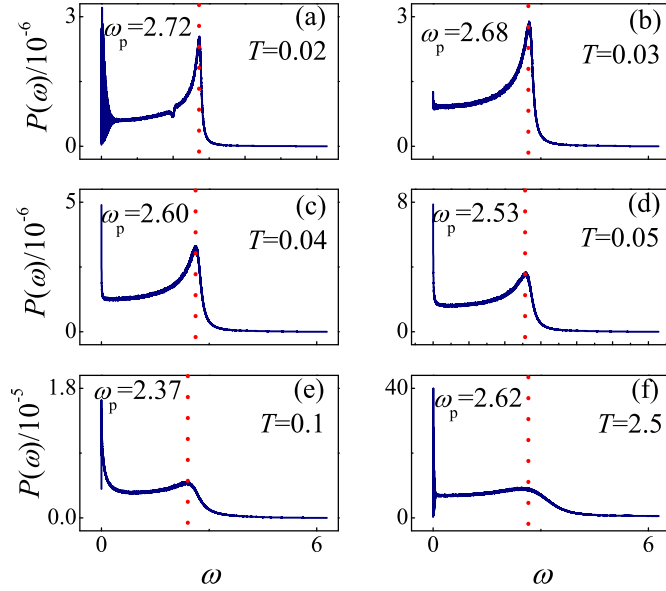


Figure 10. (Color online) Power spectra $P(\omega)$ vs T : (a) $T = 0.02$; (b) $T = 0.03$; (c) $T = 0.04$; (d) $T = 0.05$; (e) $T = 0.1$; and (f) $T = 2.5$. The dotted lines denote the peaks with frequency ω_p in the high frequency regimes.

also shows strong dependence of T , especially in some temperature ranges, phonons tend to become “softer”. These tendencies can be readily captured from the denoted peaks in high frequency regimes.

To characterize the phonons softening and to see how it is related to thermal transport, we plot the averaged frequency $\bar{\omega}$, defined by $\bar{\omega} = \int_0^\infty P(\omega) \omega d\omega / \int_0^\infty P(\omega) d\omega$, as a function of T in Figure 11. As can be seen, in addition to the turning point of $T_{tr} \simeq 0.1$ ($T_{tr} \simeq 0.05$) for heat (momentum) spreading, there is another turning point of temperature $T_{tr} \simeq 0.2$ for phonons softening. Considering that $T_{tr} \simeq 0.1$ just lies somewhere in between, we may conjecture that the observed normal heat transport is probably induced by the combined effects of viscosity from momentum spreading and the phonons softening from the spectra.

About the phonon spectra calculated here, we would also like to point out that the viscosity from momentum spreading can also be detected from phonons lowest frequency components. We address this point by using Figure 12 (a log-log plot of Figure 10). Phonons with the lowest frequency, usually called as the long-wavelength (goldstone) modes, are generally believed to be very weakly damped due to the conserved feature of momentum [46]. Because of their weak damping, the lowest frequency modes can greatly affect heat transport. From Figure 12, it can be clearly seen that with the increase of T , the damping of phonons first originates from the high frequencies and then quickly walk towards the low ones. Surprisingly we may identify that a complete damping appears around the turning temperature point of $T_{tr} \simeq 0.05$ [see Figure 12(d)], the same as that found in viscosity from momentum spreading. This result clearly indicates a strong positive correlation between the phonons damping and the viscosity from momentum

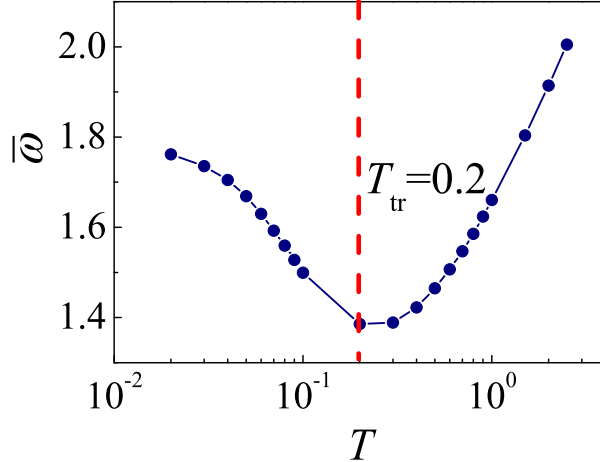


Figure 11. (Color online) The averaged frequency $\bar{\omega}$ from $P(\omega)$ vs T , where the dashed line denotes $T_{\text{tr}} = 0.2$.

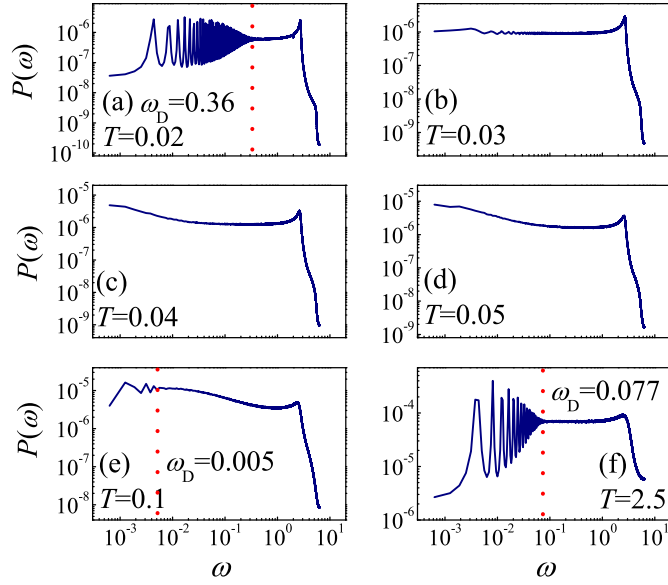


Figure 12. (Color online) Log-log plot of Fig. 10, where the dotted lines denote the frequencies ω_D below which phonons are damped very weakly.

spreading, thus implying that the origin of the long-wavelength modes may be induced by the momentum's ballistic spreading.

5. Conclusions

To summarize, we have studied in detail the heat transport behavior in the focused 1D anharmonic oscillator systems with a DW interparticle interaction like $V(\xi) = -\xi^2/2 + \xi^4/4$. By employing the equilibrium correlation method, we have captured the

PDF profile of heat spreading and precisely identified its space-time scaling property under various system temperatures. These PDF profiles are in good coincidence with Lévy walks stable distributions, and the scaling laws, for both the central part and side peaks, show good satisfactory with Lévy walks scaling as well. Based on the scaling, we have precisely presented the temperature dependent behaviors of heat transport and further verified that around the crossover temperature point of $T_{\text{tr}} \simeq 0.1$, there is a crossover from superdiffusive to normal heat transport. This result thus provides more detailed and precise numerical evidences clearly demonstrating that normal heat transport is likely to take place under the appropriate temperature regimes in the 1D systems with DW interactions, though the total momentum is conserved here.

In order to understand the mechanisms of the observed normal heat transport, we have carefully examined the spreading of other two physical quantities, i.e., the total energy and momentum. The spreading of the total energy is found to be very distinct from heat spreading. In particular, under some temperature regimes, heat can be superdiffusive while energy shows strong localizations. This unusual result thus suggests that we should take care to derive a general connection between heat conduction and energy diffusion; rather, it may be more reasonable to connect heat conduction to heat spreading.

The momentum spreading is shown to have the most viscosity around a second turning point of $T_{\text{tr}} \simeq 0.05$; however, this point of $T_{\text{tr}} \simeq 0.05$ can not directly correspond to the crossover point of heat spreading ($T_{\text{tr}} \simeq 0.1$). So to understand the observed normal heat transport, only considering the viscosity from momentum spreading is inadequate. We then perform an analysis to the phonons spectra of the system. We find that phonons tend to become softest around another turning point of $T_{\text{tr}} \simeq 0.2$. Together with the $T_{\text{tr}} \simeq 0.05$ of viscosity from momentum spreading, we then conjecture that it is the combined effects of viscosity and phonons softening that result in the normal heat transport observed in this system. All of the simulation results seem not to contradict this conjecture, though further detailed investigations remain required.

Finally, we would like to point out that, once we have understood the mechanisms, then apart from this theoretical advance, there is also room for possible applications. For example, one may be able to vary the phonons spectrum by adjusting temperatures in other DW systems, and finally manipulate heat. Such an idea would be realized by variation of the trapping frequencies in the recent focused ion chains [47]. This kind of systems has been found to exhibit a structural phase transition similar to the DW systems [48], with which then heat transport could be tunable.

Acknowledgments

D. Xiong would like to thank Profs. Hong Zhao, Jiao Wang and Yong Zhang from Xiamen university of china for their huge valuable discussions. This work was supported by the NNSF (Grants No. 11575046 and No. 11205032) of China, the NSF (Grant No. 2013J05008) of Fujian province, china.

References

- [1] Lepri S, Livi R and Politi A 2003 Thermal conduction in classical low-dimensional lattices *Phys. Rep.* **377** 1
- [2] Dhar A 2008 Heat transport in low-dimensional systems *Adv. Phys.* **57** 457
- [3] Zhong Y, Zhang Y, Wang J and Zhao H 2012 Normal heat conduction in one-dimensional momentum conserving lattices with asymmetric interactions *Phys. Rev. E* **85** 060102(R)
- [4] Chen S, Wang J, Zhang Y and Zhao H 2012 Breakdown of the power-law decay prediction of the heat current correlation in one-dimensional momentum conserving lattices arXiv:1204.5933v3
- [5] Savin A V and Kosevich Y A 2014 Thermal conductivity of molecular chains with asymmetric potentials of pair interactions *Phys. Rev. E* **89** 032102
- [6] Das S G, Dhar A and Narayan O 2014 Heat Conduction in the α - β Fermi-Pasta-Ulam Chain *J. Stat. Phys.* **154** 204
- [7] Wang L, Hu B and Li B 2013 Validity of Fourier's law in one-dimensional momentum-conserving lattices with asymmetric interparticle interactions *Phys. Rev. E* **88** 052112
- [8] Chen S, Wang J, Zhang Y and Zhao H 2013 Why asymmetric interparticle interaction can result in convergent heat conductivity arXiv:1309.7146
- [9] Xiong D, Wang J, Zhang Y and Zhao H 2012 Nonuniversal heat conduction of one-dimensional lattices *Phys. Rev. E* **85** 020102(R)
- [10] Xiong D, Zhang Y and Zhao H 2013 Heat transport enhanced by optical phonons in one-dimensional anharmonic lattices with alternating bonds *Phys. Rev. E* **88** 052128
- [11] Xiong D, Zhang Y and Zhao H 2014 Temperature dependence of heat conduction in the Fermi-Pasta-Ulam- β lattice with next-nearest-neighbor coupling *Phys. Rev. E* **90** 022117
- [12] Lee-Dadswell G R, Nickel B G and Gray C G 2005 Thermal conductivity and bulk viscosity in quartic oscillator chains *Phys. Rev. E* **72** 031202
- [13] Lee-Dadswell G R, Nickel B G and Gray C G 2008 Detailed examination of transport coefficients in cubic-plus-quartic oscillator chains *J. Stat. Phys.* **132** 1
- [14] Lee-Dadswell G R 2015 Predicting and identifying finite-size effects in current spectra of one-dimensional oscillator chains *Phys. Rev. E* **91** 032102
- [15] Popkov V, Schadschneider A, Schmidt J and Schütz G M 2015 Fibonacci family of dynamical universality classes *Proc. Natl Acad. Sci. USA* **112** 12645
- [16] Hurtado P I and Garrido P L 2015 Violation of universality in anomalous Fourier's law arXiv:1506.03234v1
- [17] Chang C W, Okawa D, Majumdar A and Zettl A 2006 Solid-state thermal rectifier *Science* **314** 1121
- [18] Giardiná C, Livi R, Politi A and Vassalli M 2000 Finite thermal conductivity in 1D Lattices *Phys. Rev. Lett.* **84** 2144
- [19] Gendelman O V and Savin A V 2000 Normal Heat Conductivity of the one-dimensional lattice with periodic potential of nearest-neighbor interaction *Phys. Rev. Lett.* **84** 2381
- [20] Li Y, Liu S, Li N, Hänggi P and Li B 2015 1D momentum-conserving systems: the conundrum of anomalous versus normal heat transport *New J. Phys.* **17** 043064
- [21] Das S G and Dhar A 2015 Role of conserved quantities in normal heat transport in one dimension arXiv:1411.5247v2
- [22] Spohn H 2014 Fluctuating hydrodynamics for a chain of nonlinearly coupled rotators arXiv:1411.3907
- [23] Roy D 2012 Crossover from Fermi-Pasta-Ulam to normal diffusive behavior in heat conduction through open anharmonic lattices *Phys. Rev. E* **86** 041102; Li H 2011 Heat conduction in one-dimensional lattice with double-well interaction *Int. Mod. Phys. B* **25** 823
- [24] Xiong D 2015 Universality or nonuniversality: Scaling for thermal transport in one dimension arXiv:1510.06540v1
- [25] Lepri S, Livi R and Politi A 1997 Heat conduction in chains of nonlinear oscillators *Phys. Rev.*

Lett. **78** 1896

- [26] Narayan O and Ramaswamy S 2002 Anomalous heat conduction in one-dimensional momentum-conserving systems *Phys. Rev. Lett.* **89** 200601; Basile G, Bernardin C and Olla S 2006 Momentum conserving model with anomalous thermal conductivity in low dimensional Systems *Phys. Rev. Lett.* **96** 204303 (2006)
- [27] Lebowitz J, Olla S and Stoltz G 2013 Final report of workshop “Nonequilibrium statistical mechanics: mathematical understanding and numerical simulation” <http://www.birs.ca/events/2012/5-day-workshops/12w5013>
- [28] Schneider T and Stoll E 1975 Observation of cluster waves and their lifetime *Phys. Rev. Lett.* **35** 296
- [29] Lee W, Kovacic G and Cai D 2013 Generation of dispersion in nondispersing nonlinear waves in thermal equilibrium *Proc. Natl. Acad. Sci. USA* **110** 3237
- [30] Denisov S, Klafter J and Urbakh M 2003 Dynamical heat channels *Phys. Rev. Lett.* **91** 194301
- [31] Cipriani P, Denisov S and Politi A 2005 From anomalous energy diffusion to Lévy walks and heat conductivity in one-dimensional systems *Phys. Rev. Lett.* **94** 244301
- [32] Zhao H 2006 Identifying diffusion processes in one-dimensional lattices in thermal equilibrium *Phys. Rev. Lett.* **96** 140602
- [33] Zaburdaev V, Denisov S and Hänggi P 2011 Perturbation spreading in many-particle systems: a random walk approach *Phys. Rev. Lett.* **106** 180601
- [34] Lepri S and Politi A 2011 Density profiles in open superdiffusive systems *Phys. Rev. E* **83** 030107 (R)
- [35] Dhar A, Saito K and Derrida B 2013 Exact solution of a Lévy walk model for anomalous heat transport *Phys. Rev. E* **87** 010103(R)
- [36] Mendl C B and Spohn H 2013 Dynamic correlators of Fermi-Pasta-Ulam chains and nonlinear fluctuating hydrodynamics *Phys. Rev. Lett.* **111** 230601
- [37] Chen S, Zhang Y, Wang J and Zhao H 2013 Diffusion of heat, energy, momentum, and mass in one-dimensional systems *Phys. Rev. E* **87** 032153
- [38] Hwang H and Zhao H 2011 Methods of exploring energy diffusion in lattices with finite temperature arXiv:1106.2866v1
- [39] Hansen J P and McDonald I R 2006 *Theory of Simple Liquids* 3rd ed (Academic, London)
- [40] Chen S, Zhang Y, Wang J and Zhao H 2013 Connection between heat diffusion and heat conduction in one-dimensional systems *Sci. China-Phys. Mech. Astron.* **56** 1466
- [41] Zaburdaev V, Denisov S and Llafter J 2015 Lévy walks *Rev. Mod. Phys.* **87** 483
- [42] Spohn H 2014 Nonlinear fluctuating hydrodynamics for anharmonic chains *J. Stat. Phys.* **154** 1191
- [43] Das S G, Dhar A, Saito K, Mendl C B and Spohn H 2014 Numerical test of hydrodynamic fluctuation theory in the Fermi-Pasta-Ulam chain *Phys. Rev. E* **90** 012124
- [44] Mendl C B and Spohn H 2014 Equilibrium time-correlation functions for one-dimensional hard-point systems *Phys. Rev. E* **90** 012147
- [45] Liu S, Xu X, Xie R, Zhang G and Li B 2012 Anomalous heat conduction and anomalous diffusion in low dimensional nanoscale systems *Eur. Phys. J. B* **85** 337
- [46] Lepri S, Livi R and Politi A 2006 *Anomalous heat conduction*, a chapter of the book “Anomalous transport: foundations and applications” edited by Klages R, Radons G and Sokolov I M
- [47] Häffner H, Roos C F and Blatt R 2008 Quantum computing with trapped ions *Phys. Rep.* **469** 155; Blatt R and Roos C F Quantum simulations with trapped ions *Nat. Phys.* **8** 277; Bermudez A, Bruderer M and Plenio M B 2013 Controlling and measuring quantum transport of heat in trapped-ion crystals *Phys. Rev. Lett.* **111** 040601
- [48] Ruiz A, Alonso D, Plenio M B and Campo A del 2014 Tuning heat transport in trapped-ion chains across a structural phase transition *Phys. Rev. B* **89** 214305; Freitas N, Martínez E and Paz J P Heat transport through ion crystals *Phys. Scr.* **91** 1